

Supplementary Information

Monovalent ion-mediated charge-charge interactions drive aggregation of surface-functionalized gold nanoparticles

Emanuele Petretto¹, Quy K. Ong², Francesca Olgiati², Mao Ting², Pablo Campomanes¹, Francesco Stellacci² and Stefano Vanni^{1*}

1. Department of Biology, University of Fribourg, Chemin du Musée 10, 1700 Fribourg, Switzerland

2. Institute of Materials, Ecole Polytechnique Federale de Lausanne, 1015 Lausanne, Switzerland

Supplementary methods

Ion density. To compute the distribution of ions around the NPs as a function of the inter-particles distance, we explored several strategies. First, we calculated the average number of cations around the NPs within the cutoff of 2.5 nm from the core center. We selected this cutoff value based on the distance where the radial distribution function of the Na⁺ around the NP core changes from adsorbed on the shell to the bulk density. This distance qualitatively represents the position of the slipping plane. Using this volume as reference, we consider three different ensembles: 1) the average number of ions around each NPs, considering all the ions (Fig. S4A); 2) the average number of ions in the union of two volume shells, thus containing the sum of all ions in either volume (Fig. S4B). 3) the average number of ions in the shared volume, i.e., the ions that the two volumes have in common (Fig. S4C).

Figure S4A shows the average number of ions around each NP as a function of NP-NP distance. Here, we can distinguish a trend that follows the same pattern shown in Fig 3F: when the two NPs are close to each other, as the number of charged ligands at the interface decrease, the ions around the NPs decrease. For NP-NP distances greater than 5 nm, the number of ions for all the systems converge to ~ 15 . Considering the sampled shell around the NPs as a unique volume, so that contains all the ions contained in either sampled sphere, the number of ions is $\sim 31 \pm 2$ for all the systems (Fig. S4B). A gentle flex is noticeable for distances larger than 5 nm, where the number of ions decreases to $\sim 28 \pm 3$, but due to the high noise, these data are to be considered qualitative. Fig S4C shows the average number of ions in the volume shared between the two NPs. This analysis shows a clear asymmetry in the ion distribution, thus clarifying the discrepancy between the number of ions reported in Fig. S4A and S4B.

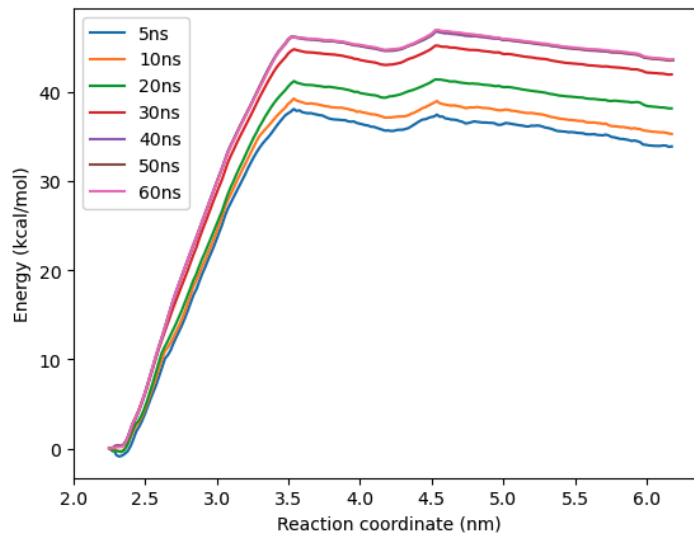


Figure S1: PMF convergence. The convergence is assessed by comparing the PMF profiles from increasing length simulation (5, 10, 20, 30, 40, 50, 60 ns).

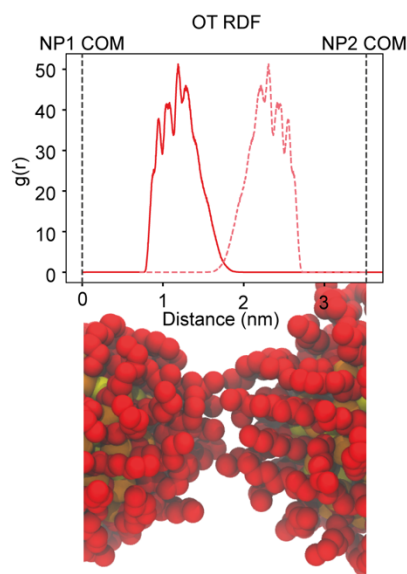


Figure S2: Radial distribution function for OT ligands and snapshot of the interacting dimer. For purely hydrophobic NPs, the PMF shows that the two NPs are completely non-interacting up to a distance of ~3.5 nm, where they start attracting each other (Figure 1A). Interestingly, this distance is comparable with the sum of two extended OT (solid line NP1, dashed line NP2).

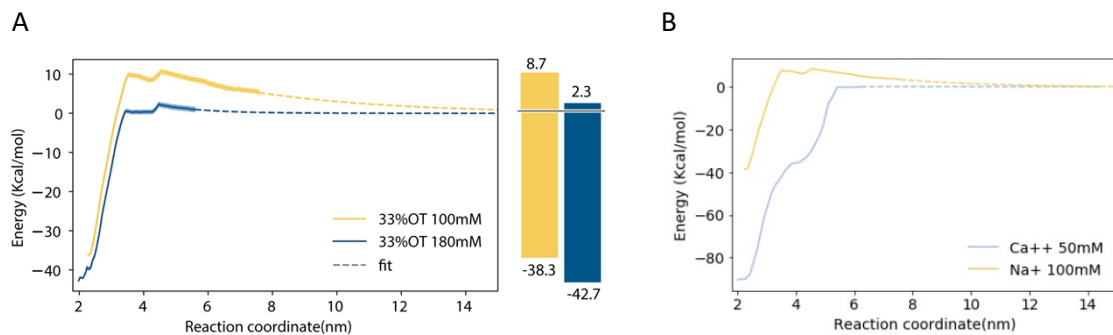


Figure S3: Effect of ion concentration and valency on the potential of mean force of NP dimerization.
A. Comparative potential of mean force of 33%OT NPs at 100 mM and 180mM ionic strengths. **B.** Comparative potential of mean force of 33%OT at Ca⁺⁺ 50 mM and Na⁺ 100mM.

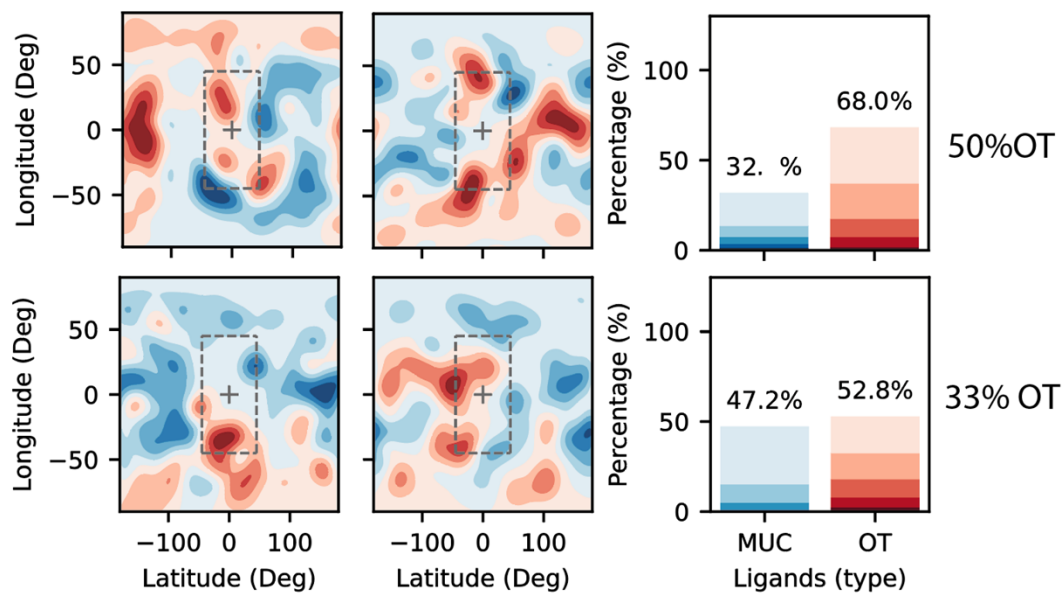


Figure S4: Comparative patterning of ligands on the surface: on top, 50%OT; on the bottom, 33%OT.

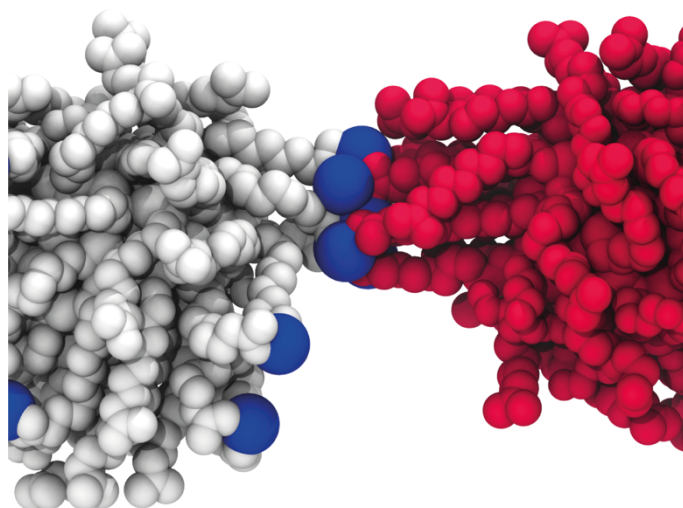


Figure S5: Snapshot of the complexes at the interface.

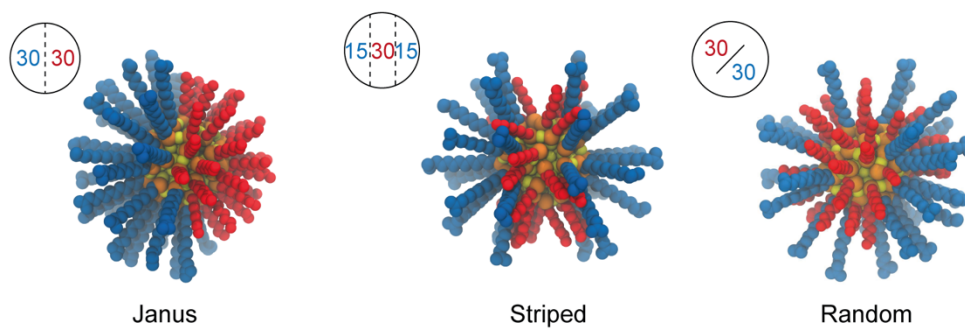


Figure S6: Structural and geometrical characteristics of patched 50% OT NPs. NPs models for Janus, Striped, and Random.

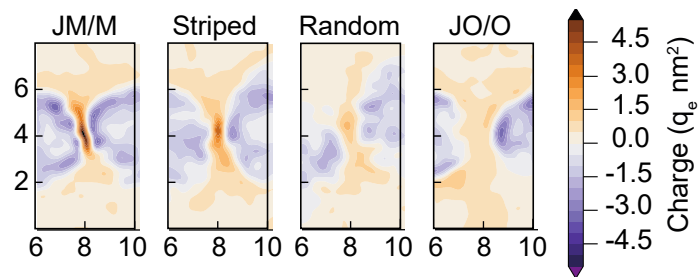


Figure S7: Detailed charge density at the NP-NP interface at 4.2 nm interparticle distance.

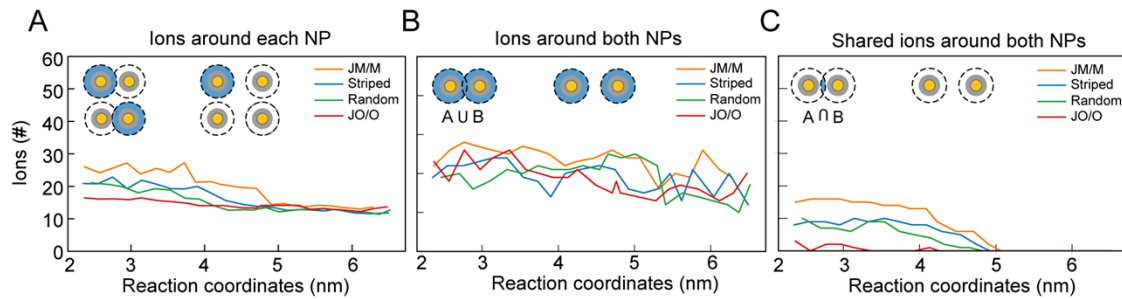


Figure S8: Ions distribution around the NPs. A. Average number of ions around each NPs, considering all the ions. B. average number of ions in the union of two volume shells. C. average number of ions in the shared volume.

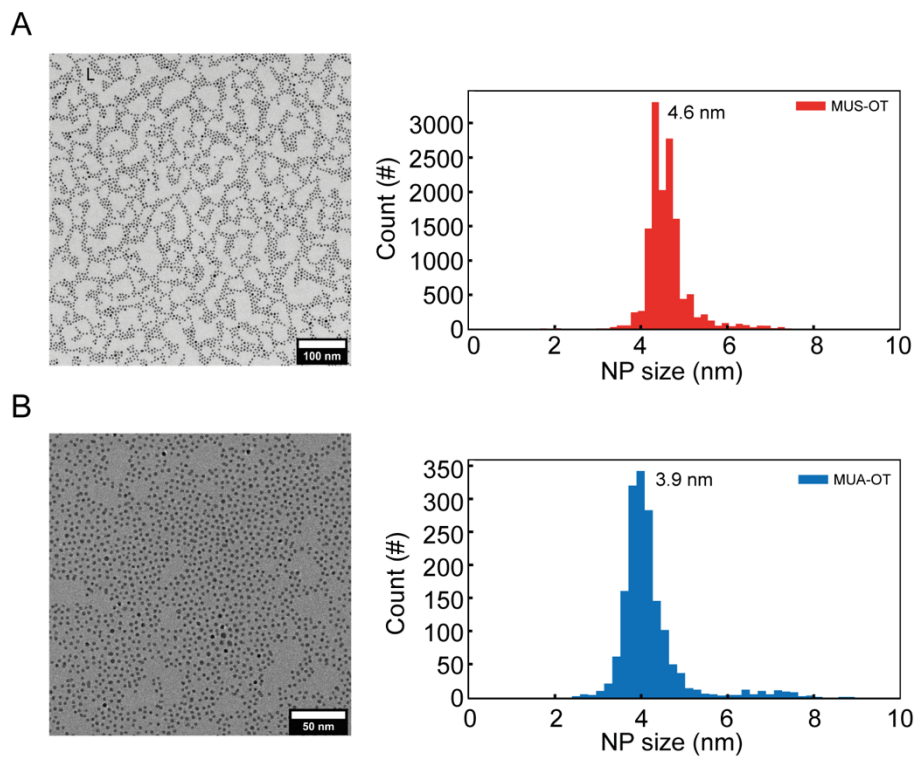


Figure S9: Size-distribution of MUA-OT and MUS-OT N